The American Journal of Pathology, Vol. 173, No. 6, December 2008

DOI: 10.2353/ajpath.2008.080234

Immunopathology and Infectious Diseases

After Injection into the Striatum, *in Vitro*-Differentiated Microglia- and Bone Marrow-Derived Dendritic Cells Can Leave the Central Nervous System via the Blood Stream

Sonja Hochmeister,* Manuel Zeitelhofer,* Jan Bauer,* Eva-Maria Nicolussi,* Marie-Therese Fischer,* Bernhard Heinke,† Edgar Selzer,‡ Hans Lassmann,* and Monika Bradl*

From the Department of Neuroimmunology, and the Department of Neurophysiology,† Center for Brain Research, Medical University Vienna, Vienna; and the Department of Radiotherapy and Radiobiology,‡ General Hospital Vienna, Vienna, Austria*

The prototypic migratory trail of tissue-resident dendritic cells (DCs) is via lymphatic drainage. Since the central nervous system (CNS) lacks classical lymphatic vessels, and antigens and cells injected into both the CNS and cerebrospinal fluid have been found in deep cervical lymph nodes, it was thought that CNS-derived DCs exclusively used the cerebrospinal fluid pathway to exit from tissues. It has become evident, however, that DCs found in peripheral organs can also leave tissues via the blood stream. To study whether DCs derived from microglia and bone marrow can also use this route of emigration from the CNS, we performed a series of experiments in which we injected genetically labeled DCs into the striata of rats. We show here that these cells migrated from the injection site to the perivascular space, integrated into the endothelial lining of the CNS vasculature, and were then present in the lumen of CNS blood vessels days after the injection. Moreover, we also found these cells in both mesenteric lymph nodes and spleens. Hence, microglia- and bone marrow-derived DCs can leave the CNS via the blood stream. ***(Am J Pathol 2008, 173:1669–1681; DOI: 10.2353/ajpath.2008.080234)***

In the intact central nervous system (CNS), dendritic cells (DCs) are contained within the meningeal and perivascular DC network, but not in the parenchyma proper.[1,2] Under pathological conditions like inflammation,[3] degeneration,[4] infection,[5] and ischemia,[6] these cells increase in numbers, mostly by immigration from the peripheral immune system, but also by differentiation of parenchymal microglial cells.[6,7] While there is ample information available about the recruitment of dendritic cells to the CNS and about their possible contribution to the exacerbation[7–9] or attenuation[6] of local immune responses, little is known about the exit of DCs from the CNS. Since brain and spinal cord lack lymphatic vessels, DCs cannot leave these organs using lymphatic drainage pathways.[10] As an alternative, emigration via cerebrospinal/interstitial fluid to deep cervical lymph nodes has been suggested.[11,12] Recently, however, it became evident that DCs found in peripheral organs can also leave their tissue via the blood stream and enter the spleen or lymph nodes.[13–21] These observations raised the questions as to whether brain-derived DCs can also leave the brain via the blood stream and whether they can migrate to peripheral lymphatic tissues. In the present study we conceived a series of experiments to specifically address these questions, and we show that microglia- and bone marrow-derived DCs can leave the CNS via the blood stream and home to mesenteric lymph nodes and spleen.

Supported by the Fonds zur Förderung der wissenschaftlichen Forschung (P16047-B02 to M.B.) and the European Commission (QLG-CT-2002-00612 to H.L.).

Sonja Hochmeister and Manuel Zeitelhofer contributed equally to this publication and should be considered first author.

Accepted for publication August 22, 2008.

Address reprint requests to Monika Bradl, Medical University Vienna, Center for Brain Research, Dept. Neuroimmunology, Spitalgasse 4, A-1090 Vienna, Austria; E-mail: monika.bradl@meduniwien.ac.at.

Materials and Methods

Animals

Lewis rats, green fluorescent protein (GFP)-transgenic Lewis rats (≥ sixth back-cross generation of the GFP transgene onto the Lewis rat background) and Sprague-Dawley rats were used throughout this study. They were bred at the Decentral Facilities of the Institute for Biomedical Research (Medical University Vienna).

Microglial Cultures

Microglial cultures were established essentially as described.[22] Briefly, 0 to 1 day old GFP-transgenic and wild-type Lewis rats were sacrificed and their brains dissected. For each culture, the brains of 8 to 12 rats were dissociated in 2 to 3 ml of 1× trypsin. The resulting single cell suspensions were cultured for 5 to 7 days in poly-L-lysine-coated culture dishes, using RPMI 1640/10% fetal calf serum, and changing the medium every other day. After this time period, the mixed glial cell cultures consisted of a monolayer of astrocytes and some fibroblasts. On top of this monolayer, ramified microglial cells and glial progenitor cells were found. These cells were only loosely adherent. They were detached by shaking confluent mixed glial cultures for 12 to 15 hours (180 rpm, 37°C) and then plated for 5 to 10 minutes onto fresh, uncoated culture dishes. This led to the selective adherence of microglial cells, which were now no longer ramified, but had an amoeboid, macrophage-like phenotype. All other glial cells could not adhere and were removed by subsequent, vigorous washing in PBS. The resulting microglial cultures routinely had a purity of >99%. On average, 2 to 3 shake-offs, separated by 3 to 5 days, could be prepared from each mixed glial culture. For our studies, cells of the first through third shake-off were used.

Differentiation of Microglial Cells along the DC Lineage

Microglial cultures were supplemented with 10 ng/ml each of recombinant rat granulocyte/monocyte colony stimulating factor (GM-CSF) and recombinant rat interleukin 4 (IL-4; all RnD Systems, Wiesbaden, Germany). Treatment of microglial cells with these factors changed the morphology of the microglial cells to a spindle-shaped phenotype. After 7 to 13 days of culture, micDCs detached from the adherent cell layer and were harvested from the supernatant of these cultures.

Discrimination between Cells Derived from the Microglia or the Meningeal/Perivascular Cell Pool with Bone Marrow Chimeric Rats

Four to eight-week-old Lewis rats were irradiated (10 Gray) and immediately afterward injected i.p. with bone marrow cells derived from GFP-transgenic Lewis rats. For microglial cultures, these chimeric animals were sacrificed 4 to 15 months after bone marrow transfer. At the same time point, blood was taken to determine the degree of chimerism (= percentage of GFP-labeled white blood cells in the total white blood cell pool). The resulting microglial cells were then differentiated with GM-CSF/IL-4, and the percentage of GFP^+ micDCs in the cell population with a morphological DC phenotype was determined by two different observers. One of these observers was blinded to the experiment.

Differentiation of Bone Marrow Cells along the DC Lineage

Bone marrow derived-DCs (bmDCs) were essentially generated as described,[23] using RPMI 1640/fetal calf serum containing 10 ng/ml each of recombinant rat GM-CSF and recombinant IL-4. BmDCs were harvested from these cultures after 7 to 13 days.

Characterization of MicDCs and BmDCs

Analysis of Surface Marker Expression by Flow Cytometry

For staining, the cells were incubated for 30 minutes at 4°C with antibodies against rat MHC class I (OX18), MHC class II (OX6), CD11b (OX42), CD11c, CD80 (B7.1), CD86 (B7.2), CD54 (intercellular adhesion molecule-1 [ICAM-1]), CD8α (OX8), CD4 (W3/25), and OX62 antigen (all from Serotec, Düsseldorf, Germany), diluted 1:100 in stain buffer (BD Pharmingen, San Diego, CA). Isotype matched control antibodies, mouse IgG1 and IgG2a (both from Dako, Glostrup, Denmark) were used. The cells were washed in stain buffer and incubated for 30 minutes at 4°C with polyclonal goat anti-mouse IgG-FITC (F[ab′]2, Dako, for wild-type cells) or polyclonal goat-anti-mouse IgG-RPE (F[ab′]2, Dako, for GFP-transgenic cells).

Analysis of Antigen Capture

MicDCs and bmDCs were cultured for 30 minutes in the presence of 100 μg/ml fluorescein isothiocyanate (FITC)-dextran or 0.2 μg/ml FITC-bovine serum albumin [BSA] (both from Sigma, Vienna, Austria), or 100 μg/ml fluorescein-conjugated *E. coli* K12 bioparticles (FITC-K12; Molecular Probes/Invitrogen, Glasgow, Scotland, UK). One aliquot of these cells was incubated at 4°C (control, to reveal unspecific binding of FITC-dextran or FITC-BSA), the other at 37°C (to reveal antigen capture and uptake). Antigen uptake was stopped by washing in ice-cold stain buffer, and evaluated by flow cytometry or fluorescence microscopy.

Analysis of the Response to Lipopolysaccharide

MicDCs and bmDCs were used after 7 days of differentiation in GM-CSF/IL-4 containing medium. Then, the cul-

ture was continued for 48 hours in the presence (experimental cells) or absence (controls) of 100 ng/ml lipopolysaccharaide (LPS; from *E. coli* 0127:B8, Sigma). The surface properties of cells from both groups were characterized by flow cytometry.

Mixed Lymphocyte Reactions

MicDCs and bmDCs were used 7 to 12 days after initiation of differentiation with GM-CSF/IL-4. T cells were isolated from the mesenteric lymph nodes of Sprague-Dawley rats. Graded doses of micDCs or bmDCs and T cells were cocultured as triplicates in a total volume of 200 μl. The DC:T cell ratios ranged from 0.5:1 to 0.0125:1. For the last 18 hours of a 48 hours incubation, [^{3}H]-thymidine was added. The cells were harvested onto glass fiber filter membranes and the [^{3}H]-thymidine incorporation was measured in a β-counter.

Transcription Factor Usage

cDNA from micDCs or bmDCs was used for PCR analysis, using primers specific for PU.1 (PU.1-for: 5′-TGGAAGGGTTTCCCCTCGTC-3′; PU.1-rev: 5′-TGCTGTCCTTCATGTCGCCG-3′; product 533 bp), Spi-B (Spi-B-for: 5′-GGCTTCG GTTTTTGAGATTGGG-3′; Spi-B-rev: 5′-TGACTGTAAAAGGGGGCTTTCC-3′; product 381 bp), and β-actin (β-act-for: 5′-ATGAAGTGTGACGTTGACATCC-3′; β-act-rev: 5′-GCCAGCTCAGTAACAGTCCGCC-3′; product 303 bp). For PCR reactions, 5 μl 10× PCR buffer (200 mmol/L Tris-HCl, pH 8.4, 500 mmol/L KCl), 1.5 μl 50 mmol/L $MgCl_2$, 1 μl 10 mmol/L dNTP mix, 1 μl forward primer (100pmol/μl), 1 μl reverse primer (100pmol/μl), 1 μl Hot Gold Star polymerase (5U/μl, Eurogentec, Seraing, Belgium), 1 μl cDNA, and 38.5 μl H_2O were mixed, heated for 11 minutes at 95°C (denaturation), and then subjected to 40 cycles of denaturation (30 seconds, 95°C), annealing (30s, 56°C for PU.1; 55°C for Spi-B; 53°C for β-act) and elongation (30s, 72°C). The MyCycler Thermal Cycler system with thermal gradient (Bio-Rad, München, Germany) was used. Final extension was made for 10 minutes at 72°C. The resulting PCR products were size-separated by agarose gel electrophoresis, excised, and sequenced.

Microarrays

Oligo GEArray rat inflammatory cytokines & receptors microarrays and oligo GEArray rat chemokines & receptors microarrays (all from SuperArray, Frederick, MD) were used according to the instruction of the manufacturer.

Injection of GFP$^+$ Cells into the Striata of Wild-Type Lewis Rats

Six-week-old wild-type Lewis rats were anesthetized with Ketanest S/Rompun and placed in a stereotactic head frame. The incisor bar was adjusted until the plane defined by the lambda and bregma was parallel to the base plate. Then, the needle of a 0.5 μl Hamilton syringe was stereotactically guided into the left striatum (3 mm lateral to bregma, 4 mm below the dura). 0.3 μl solution (containing ~10000 GFP$^+$ cells) in sterile endotoxin-free PBS was slowly injected. The needle was left in place for an additional 10 minutes before it was removed. The animals were sacrificed 0.5, 1, 3, and 6 days later for histological analyses. Initially, we used GFP$^+$ micDCs after 7 days of differentiation, or after 7 days of differentiation and an additional stimulation for 48 hours with TNF-α to obtain more mature cells. Since both types of cells showed an absolute identical migratory behavior, we refer to them as one single group. All animal experiments were approved by the local animal welfare committee and the Austrian Ministry for Education, Science, and Culture.

Histological Analysis

For histological examination, the animals were euthanized with CO_2 and then perfused with 4% paraformaldehyde in phosphate buffered saline pH 7.4. The brains, lymph nodes and spleens were dissected, postfixed in paraformaldehyde/PBS and paraffin-embedded. Serial sections were cut on a microtome. Antigen was retrieved by steaming the tissue sections in 1 mmol/L citric acid buffer pH 6.0 (for usage in double stainings with Ox6 and CM1) or 1 mmol/L EDTA buffer, pH 8.5 (all other antibodies and antibody combinations) for 60 minutes. Immunohistochemical staining and confocal microscopy were done as described,[24] using rabbit anti-GFP antibodies (gift of W. Sieghart, Med. University Vienna, Center for Brain Research), mouse anti-rat MHCII (OX6), rabbit anti-activated caspase 3 (CM-1, antibody kindly provided by Thomas Deckwerth, Idun Pharmaceuticals, San Diego, CA), mouse anti-rat T cells (W3/13), and rabbit anti-human von Willebrand factor (vWF, cross-reactive with rat, DAKO, Glostrup, Denmark) as primary antibodies.

For the detection of apoptotic cells, tissue sections were pretreated with 1 mmol/L citric acid buffer, and then incubated over night at 4°C with OX-6 (1:250) and CM-1 (1:50,000). Bound OX-6 was detected by alkaline phosphatase conjugated anti-mouse IgG (1:200) followed by Fast Blue B base (Sigma), and bound CM-1 was visualized using biotinylated donkey-anti-rabbit (Amersham Pharmacia Biotech, Uppsala, Sweden) in fetal calf serum/PBS (1 hour, room temperature) followed by avidin peroxidase (1:100; Sigma; 1 hour, room temperature) and stained with 3,3′diaminobenzidine-tetra-hydrochloride (Sigma). Sections were inspected using conventional light microscopy.

For determining the location of injected cells, double-staining was performed with OX6 (1:100) and anti-vWF (1:500), which were applied over night at 4°C. Bound OX6 was detected with a donkey anti-mouse Cy2 (green), bound anti-vWF antibodies with biotinylated sheep anti-rabbit antibodies (Amersham Pharmacia Biotech, 1:200) and then with streptavidin-Cy3 (red) (Jackson Immuno Research Laboratories, West Grove, PA, 1:75). Alternatively, anti-GFP (1:2500) and anti-vWF (1:

500) antibodies were applied over night at 4°C. Bound anti-vWF antibodies were detected with goat anti-rabbit Cy3 (Jackson Immuno Research Laboratories, 1:100). Since they also reacted with the biotinylated sheep anti-rabbit antibodies (1:200) and the streptavidin-Cy2 (Jackson Immuno Research Laboratories, 1:75) used to detect bound anti-GFP antibodies, blood vessel endothelium appears yellow, and GFP^+ cells green. Sections were inspected with a laser confocal microscope (LSM-410, Carl Zeiss, Jena, Germany).

PCR Analysis of Lymphatic Tissue to Verify the Presence of GFP^+ micDCs

We isolated RNA from paraformaldehyde-fixed paraffin embedded tissue sections from mesenteric lymph nodes and spleens, using the Paradise Whole Transcript RT Reagent System (Arcturus, Mountain View, CA) according to the instructions of the manufacturer. This RNA was transcribed to cDNA and then subjected to PCR analysis, using primers specific for GFP (GFP-for: 5′-GCTGACCCTGAAGTTCATCTGC-3′; GFP-rev: 5′-GTGGCTGTTGTAGTTGTACTCC-3′; product 302 bp), and β-actin. For PCR reactions, 5 μl 10× PCR buffer (200 mmol/L Tris-HCl, pH 8.4, 500 mmol/L KCl), 1.5 μl 50 mmol/L MgCl2, 1 μl 10 mmol/L dNTP mix, 1 μl forward primer (100pmol/μl), 1 μl reverse primer (100pmol/μl), 1 μl polymerase (5U/μl), 1 μl cDNA, and 38.5 μl H_2O were mixed together. The reaction mix was heated for 11 minutes at 95°C (denaturation), and then subjected to 40 cycles of denaturation (30s, 95°C), annealing (30s, 55°C for GFP; 53°C for β-act) and elongation (30s, 72°C). The final extension was made for 10 minutes at 72°C. The size of the resulting PCR products was determined by agarose gel electrophoresis. Afterward, the PCR products were purified and sequenced.

T Cells

All T cells used were memory T cells specific for myelin basic protein (MBP, Sigma), derived from Lewis rats, and were "resting," ie, readily activatable in response to MBP and syngenic antigen presenting cells.

T Cell Labeling

We used the Vybrant CFDA SE Cell tracer kit (Invitrogen, Lofer, Austria) to obtain carboxyfluorescein succinimidyl ester (CFSE)-labeled MBP-specific T cells, and CellTracker Orange 5- and-6-[4-chloromethyl] benzoyl amino (CMTMR) tetramethylrhodamine (Invitrogen) to obtain CellTracker Orange labeled MBP-specific T cells. In both cases, the labeling procedure followed the instructions of the manufacturer.

Search for Proliferation of CFSE-Labeled MBP-Specific T Cells by FACS

GFP^+ microglia-derived dendritic cells in 1 ml culture medium were pre-incubated for 45′at 37°C with 10 μl MBP as the cognate or 10 μl Ovalbumin (Sigma) as an irrelevant antigen. The stock concentrations of the antigens used were 1 mg/ml. After the incubation, the cells were carefully washed to remove any traces of unbound antigens. Then, ~10,000 GFP^+ microglia-derived dendritic cells per rat were injected into the striatum, as outlined in the material and methods section. Two rats per group were injected. Immediately after the intrastriatal injection of the antigen-loaded dendritic cells, 2.5×10^6 CFSE-labeled and 2.5×10^6 unlabeled resting MBP-specific T cells were injected i.p./i.v. Six days later, splenocytes of these animals were analyzed by flow cytometry to search for proliferation of CFSE-labeled T cells. Remaining splenocytes were used for ELISPOTS and T cell proliferation assays.

Search for Expansion of MBP-Specific T Cells by ELISPOT Analyses and T Cell Proliferation Assays

ELISPOT analyses were performed on spleens of Lewis rats that had been injected with GFP^+ MBP- or ovalbumin-loaded microglia-derived dendritic cells into the striatum, and with CFSE-labeled and unlabeled resting MBP-specific T cells i.p./i.v. (see above). Six days after these manipulations, the animals were sacrificed, and 1.25, 2.5, 5, and 10×10^4 erythrocyte-depleted splenocytes were seeded in triplicate in the absence of any antigen (negative control), or in the presence of MBP, OVA (both final concentration 10 μg/100 μl), or Concanavalin A (ConA, Sigma, final concentration 2.5 μg/100 μl, positive control), using the rat interferon-γ ELISPOT (U-CyTech, Utrecht, Netherlands) according to the instructions of the manufacturer. For T cell proliferation assays, 1×10^6 erythrocyte-depleted splenocytes/well were seeded in triplicate in the absence of any antigen (negative control), or in the presence of MBP, OVA (both final concentration 10 μg/100 μl), or ConA (final concentration 2.5 μg/100 μl, positive control). The cells were cultured for 72 hours. [^{3}H]-thymidine was added during the last 18 hours of culture to reveal *de novo* DNA synthesis during the S-phase of the cell cycle of activated T cells.

Search for Direct Physical Interaction between CellTracker Orange Labeled MBP-Specific T Cells and GFP^+ Emigrated micDCs in the Spleen

Approximately 10,000 microglia-derived GFP^+ dendritic cells/rat were injected into the striatum of five Lewis rats, as outlined in the material and methods section. 0.5 to 1×10^7 resting CellTracker Orange labeled MBP-specific T cells were immediately afterward injected i.p./i.v. The animals were sacrificed 1 (2 rats), 2 (2 rats), or 3 days (1 rat) after the injection, and perfused with 4% paraformaldehyde. Cryosections of the spleens were made and analyzed by confocal microscopy.

Results

Generation and Characterization of micDCs

To initiate the differentiation to DCs, the shake-offs of mixed glial cultures were cultured in the presence of 10 ng/ml GM-CSF and IL-4. Seven to thirteen days later, these cultures consisted of large adherent, macrophage-like cells, and of freely floating, smaller cells with processes suggestive of DCs. Since there was no good antibody marker available that unequivocally identifies rat DCs, we characterized the floating cells according to their morphology, surface marker expression, response to LPS, and ability to activate naive T cells.

All of these cells had cellular processes of variable length (Figure 1A) and were CD11c$^+$, CD11b$^+$, ICAM-1$^+$, B7.1$^+$, and B7.2$^+$ (Figure 1B). The expression of the OX62 antigen was inconsistent, ranging from a complete or near-complete absence (in 56%) to moderate (in 13%) to high levels (in 31% of all cultures, data not shown). Even in the absence of additional maturation stimuli such as LPS, these cells expressed large amounts of MHC class II products and costimulatory molecules on the cell surface (Figure 1B) and were able to activate naive T cells (Figure 1C). They efficiently took up FITC-dextrane and FITC-BSA, but showed only surface-binding of FITC-K12 (Figure 1D), while undifferentiated microglial cells readily took up FITC-dextrane, FITC-BSA, and FITC-K12 (Figure 1E).

Rat cells with such a phenotype have been called DCs previously.[25] However, since there is currently no marker available that unequivocally shows whether such differentiated cells are really of the DC lineage, or whether they provide an independent myeloid lineage, we rather prefer to term these cells "DC-like."

Different subsets of murine[26] and rat[27] DCs can be readily distinguished by their expression of CD8α. We therefore characterized the expression of CD8α molecules on the surface of micDCs by FACS analysis. Twenty-four of 28 independent cultures gave rise to CD8α^- micDCs. In 4/28 cultures, pure populations of CD8α^+ micDCs were obtained. The differentiation of microglial cells to CD8α^- and CD8α^+ micDCs reflects the normal differentiation pattern of myeloid DCs in mice and rats. In these species, both CD8α^- and CD8α^+ myeloid DCs can derive from the same precursor cell,[26,28] and do not change their CD8α status *in vitro*.[29] To further characterize the micDCs, we determined their transcription factor profile by PCR analysis. We concentrated on the transcription factors PU.1 (typically used by myeloid DCs[30,31]), and Spi-B (used by plasmacytoid DCs[32,33]). We found that the micDCs used PU.1, but not Spi-B (Figure 1F). In a subsequent step, we characterized the cytokine/chemokine expression profile of the micDCs by pathway-focused microarrays. In contrast to microglial cells, micDCs expressed significantly more transcripts for CCL17 and CCL 22, while the expression of IL-12α and IL-12β was below the limit of detection with this technology (Figure 1G). These are typical features of semimature dendritic cells.[34] We then treated the micDCs *in vitro* with the maturation stimulus LPS. The cells responded to LPS and were able to further up-regulate the surface expression of B7.1, B7.2, ICAM-1, or MHC class II molecules (Figure 1H). However, we rarely observed an up-regulation of all markers at the same time. Again, this phenotype strongly suggests that the micDCs were semimature.

Cell Cultures Derived from Bone Marrow Chimeric Rats Reveal the True Microglial Origin of GM-CSF/IL-4–Differentiated MicDCs

Conventionally, the myeloid cells found within the first through third shake-offs of mixed glial cultures are considered microglial cells.[22] Moreover, cells derived from the different shake-offs are known to have a comparable *in vitro* phenotype, based on the phagocytic ability, morphology, specific immunoreactivity, cytokine secretion, and LPS response.[35] However, there was still the possibility that our shake-offs also contained blood mononuclear cells that had been trapped in the vasculature, or dendritic/myeloid cells initially located in the perivascular or meningeal compartments,[1,2,36] and that the GM-CSF/IL-4–recruited micDCs derived from these cellular sources. To clarify this issue, we produced bone marrow chimeras by injecting hematopoietic stem cells of GFP-transgenic Lewis rats into irradiated wild-type Lewis rats. The resulting animals were characterized by a high degree of chimerism (on average 80% to 87% of all peripheral blood mononuclear cells were GFP$^+$), by the presence of GFP$^+$ mononuclear cells in the meninges and in the perivascular spaces, and by a GFP$^-$ microglial cell pool (Figure 2A) that remained stably GFP$^-$ throughout life (data not shown). We then used these animals to initiate mixed glial cultures as starting material for the production of GM-CSF/IL-4 differentiated micDCs, as done before for newborn rats. From these cultures we obtained too few micDCs for full characterization of the cells. Despite these difficulties, we were able to verify that these cells were able to activate naive T cells and had the typical morphology of micDCs (data not shown), and we determined then the presence or absence of GFP in these cells by fluorescence microscopy. We found that the vast majority of these chimera-derived micDCs was GFP$^-$. This finding is in clear contrast to the situation in the peripheral blood, where most nucleated cells carried the genetic marker (Figure 2B). To make sure that the large numbers of GFP$^-$ cells did not reflect any deleterious effects of the GFP transgene on microglial cell growth and differentiation, we initiated mixed glial cultures by pooling equal numbers of brains from 3 GFP$^-$ and 3 GFP$^+$ Lewis rat pups, and determined the ratios of GFP$^+$ and GFP$^-$ micDCs derived from such cultures. We found that both types of micDCs were present in comparable numbers (Figure 2C). This indicated that GFP$^+$ and GFP$^-$ cells grew and differentiated equally well in culture.

Collectively, these data imply that GM-CSF/IL-4 differentiated cells obtained from the shake-offs of mixed glial cultures can originate in the microglial cell pool, although we cannot fully exclude the possibility that some DCs from these cultures also derived from a GFP$^-$, slowly

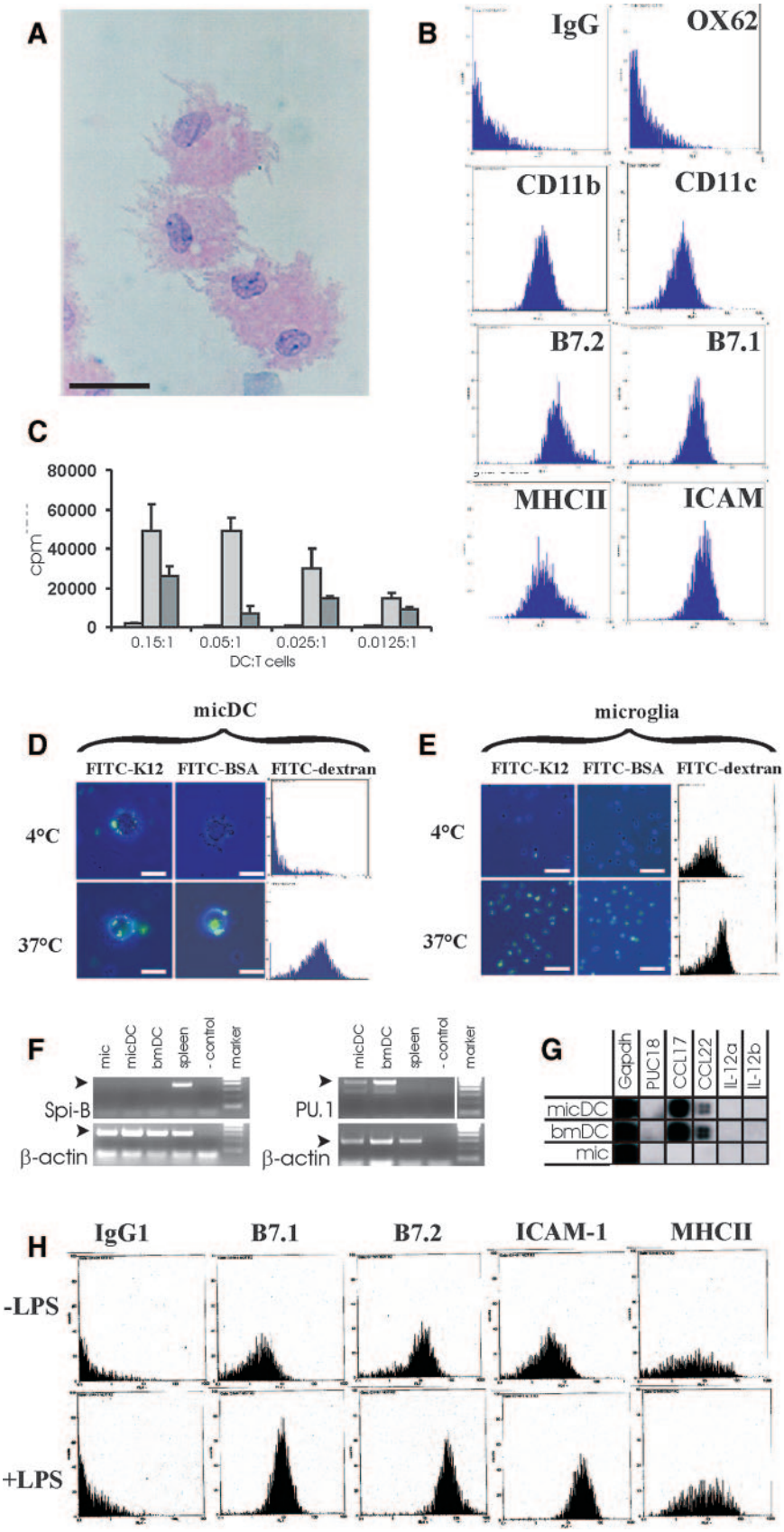

Figure 1. Characterization of micDCs. Microglial cultures were treated for 7 to 13 days with GM-CSF and IL-4. The non-adherent, free-floating cells were harvested and characterized according to morphological appearance (**A**), surface marker expression revealed by flow cytometry (**B**), ability to activate naïve T cells in mixed lymphocyte reactions (**C**), ability to take up antigens (**D, E**), transcription factor usage (**F**), expression of chemokines/cytokines (**G**), and response to activation by LPS. **A:** MicDCs have a round, irregular morphology with many dendrites and protrusions of variable length. **B:** Flow cytometric analysis of surface marker expression reveal the expression of costimulatory molecules (B7.1 and B7.2), the ICAM, and CD11b and CD11c. The expression of the OX62 antigen was inconsistent, ranging from a complete or near-complete absence (in 56%) to moderate (in 13%) to high levels (in 31% of all cultures). The high expression of surface MHC class II indicates that these micDCs are no longer immature. These data are representative of 28 independent cultures. **C:** MicDCs can activate naïve T cells, as demonstrated in mixed lymphocyte reactions where micDCs were derived from Lewis rats, and T cells from mesenteric lymph nodes of Sprague-Dawley rats. Different DC:T cell ratios were tested. The white box represents microglial cells harvested from mixed glial cultures, and the gray and black boxes represent two different cultures of micDCs. Counts per minute (cpm) ± standard deviations are shown. This experiment is representative of six independently derived micDCs preparations. **D, E:** Fluorescent microscopy or FACS images from micDCs (**D**) or microglial cells (**E**) treated with FITC-K12, FITC-BSA, and FITC-dextran at 4°C (to reveal nonspecific binding) and at 37°C (to show true uptake). Data are representative of several different experiments. **F:** Transcription factor profile of micDCs compared to microglial cells and bmDCs. MicDCs and bmDCs express PU.1 but not Spi-B and therefore resemble myeloid DCs. **G:** Pathway-focused rat inflammatory cytokines microarrays. mRNA from micDCs, bmDCs, and microglial cells (mic) were screened for the presence for transcripts encoding CCL17, CCL22, IL-12a, IL-12b. Glyceraldehyde-3-phosphate dehydrogenase (GAPDH) transcripts were used as a positive control. A PUC18 plasmid was used as a negative control. Please note that the greyish hue in the PUC18 sample results from a strong signal next to this probe. The data shown here are representative of two independently performed experiments. **H:** MicDCs *in vitro* are still able to respond to LPS and up-regulate the surface expression of B7.1, B7.2, ICAM-1, or MHC class II. Please note that we rarely observed an up-regulation of all markers, probably since we did not compare immature with mature DCs, but rather semimature with mature DCs. In 1/9 cultures analyzed, the most extreme case was observed, with an up-regulation of MHC-class II gene products together with CD11b, CD11c, B7.1, B7.2 and OX62 (shown in **A**). In other cultures, the response to LPS was much less pronounced, resulting in an up-regulation of CD11b and CD11c either alone (2/9 cultures) or together with B7.1 (2/9 cultures). B7.1 was up-regulated alone in 1/9 cultures. ICAM-1 was up-regulated together with OX62 (1/9 cultures), or with B7.1 and B7.2 (2/9 cultures). This indicates that the cells treated with LPS were already semimature. Bars = 25 μm (**A, D**) and 50 μm (**E**).

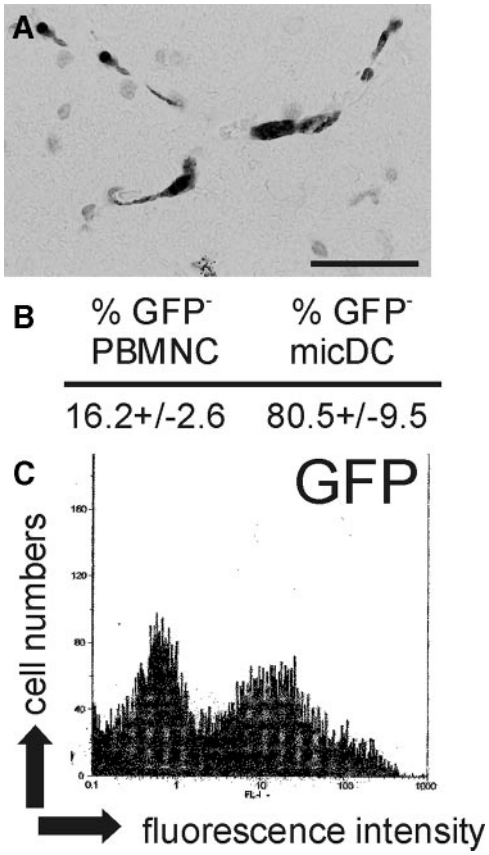

Figure 2. Combined *in vivo* and *in vitro* study to reveal the microglial origin of micDCs. **A:** Histological analysis of brain and spinal cord sections with anti-GFP antibodies. GFP^+ bone marrow derived cells (dark) are seen in perivascular areas, but not in the parenchymal microglial cell pool. Scale bar = 50 μm. **B:** Percentages of GFP^+ cells in the micDC population. Shown here are the mean values (± SD) of six different bone marrow chimeric rats. Note that the percentage of GFP^- cells in the micDC pool is much higher than the percentage of GFP^- cells in the pool of peripheral blood mononuclear cells (PBMNC) indicating that most of the GFP^- micDCs must derive from the GFP^- microglial cell pool. **C:** FACS-analysis of micDCs that had been derived from a mixed glial culture prepared from three GFP^+ and three GFP^- pups. Note that similar amounts of GFP^+ and GFP^- micDCs are present, which indicates that both cellular subsets grow equally well in culture. Data shown here are representative of two independently performed experiments.

exchanging perivascular precursor cell population co-isolated from the brain.

MicDCs Do Not Differ from BmDCs, but Both Differ from Microglial Cells

Based on the expression of CD11c, CD11b, ICAM-1, B7.1, B7.2, and MHC class II gene products (Figure 3A), on the LPS response and the ability to activate naive T cells (data not shown), and on the transcription factor usage and CCL17/CCL22 expression pattern (Figure 1), bmDCs were indistinguishable from their microglia-derived counterparts. Both micDCs and bmDCs, however, differed significantly from microglial cells in surface marker expression (Figure 3B), ability to activate naive T cells (Figure 1C), and expression levels of CCL17/CCL22 mRNA (Figure 1E).

MicDCs Derived from GFP-Transgenic Lewis Rat Brains Have the Same Characteristics as their Lewis Rat-Derived Counterparts

To study the fate of micDCs *in vivo*, we produced GFP^+ micDCs. Like their unlabeled counterparts, these cells expressed MHC class II products on the cell surface, together with ICAM-1 and the costimulatory molecules B7.1 and B7.2 (Figure 3C). They also expressed CCL17 and CCL22, and were able to activate naive T cells (data not shown).

Migration of micDCs within and Out of the Brain

We then injected the GFP^+ micDCs into the striatum. Shortly after the injection, the GFP^+ micDCs were found in the needle tract and in the surrounding parenchyma (Figure 4, A–C). However, over time, the total number of micDCs found in these locations decreased. This was in part due to the induction of apoptosis (3 days after the injection, 3.0% of all $Ox6^+$ micDCs were apoptotic according to their reaction with the caspase 3 antibody; other evidence for apoptosis = the condensation or fragmentation of nuclei depicted in Figure 4 days), and in part due to the migration of micDCs from the CNS parenchyma to the perivascular space (Figure 4, E and F). Even 72 hours after the injection, we found micDCs that had integrated between the endothelial layer of the vasculature and directly contacted the lumen of the blood vessels (Figure 4, G–I), and we detected micDCs within the blood vessel lumen (Figure 4J). Hence, micDCs are able to leave the CNS compartment and to enter the circulation.

MicDCs that Had Left the Brain via the Blood Stream Reach the Mesenteric Lymph Nodes and the Spleen

We then searched for GFP^+ micDCs in the peripheral lymphatic organs. We found these cells in very low numbers in the white pulp of the spleen, just at the border to the red pulp (Figure 5A), and in the medulla of mesenteric lymph nodes (Figure 5B). These findings were further corroborated by the presence of GFP mRNA in these organs (Figure 5C).

BmDCs Behave Essentially Like their Microglia-Derived Counterparts

The experiments described above raised the question whether the emigration from the CNS parenchyma is a typical feature of micDCs, or whether it is also seen on injection of bmDCs into the striatum. To address this point, we derived GFP^+ DCs from the bone marrow of GFP-transgenic Lewis rats (Figure 6A), and injected these cells into the striatum of wild-type Lewis rats. As seen before for micDCs, GFP^+ bmDCs were found in the CNS parenchyma (Figure 6B). Some of these cells became apoptotic (3 days after the injection, 5.6% of the bmDCs were apoptotic according to their staining with the caspase 3 antibody; other evidence for apoptosis = the

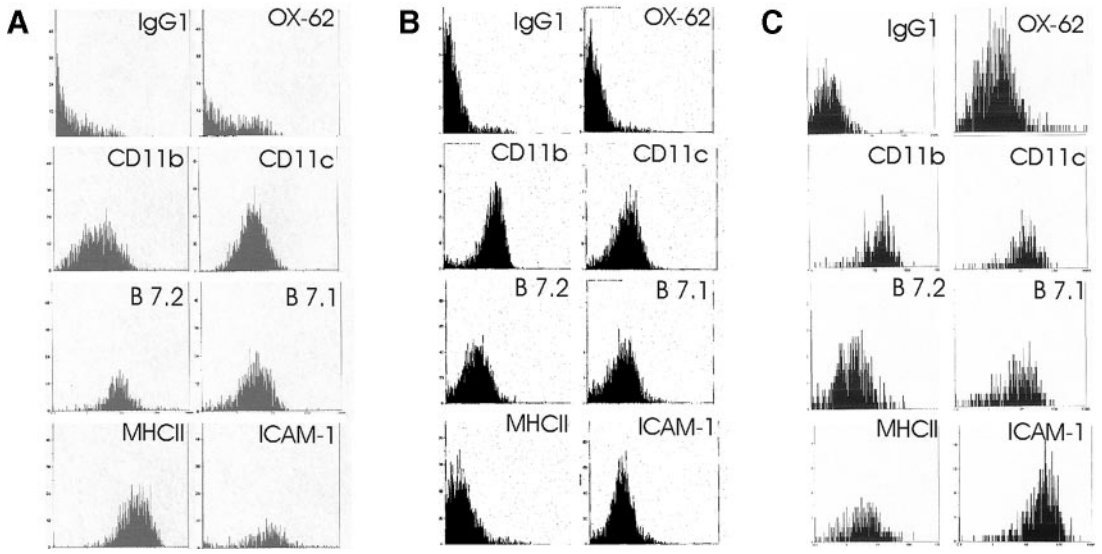

Figure 3. Flow cytometric analysis of surface marker expression. BmDCs (**A**), microglial cells (**B**), and GFP$^+$ micDCs (**C**) were analyzed. Both bmDCs and micDCs are characterized by a strong surface expression of MHC class II products and ICAM-1, which is not seen on microglial cells. These data are representative of five bmDC, five microglial, and two GFP$^+$ micDC cultures.

condensation or fragmentation of nuclei shown in Figure 6C), while others were found in the perivascular space (Figure 6 days), and even within the blood vessel lumen (Figure 6E). Finally, we found some of these cells in the spleen (Figure 6, F and G). This indicated that bmDCs are also able to leave the CNS parenchyma and to enter lymphoid organs.

Emigration Is Not Observed on Injection of GFP$^+$ Microglial Cells

In a next series of experiments, we had to exclude the possibility that the micDCs or bmDCs were introduced into the perivascular space and/or the blood vessel lumen by the injection procedure itself. Therefore, we iso-

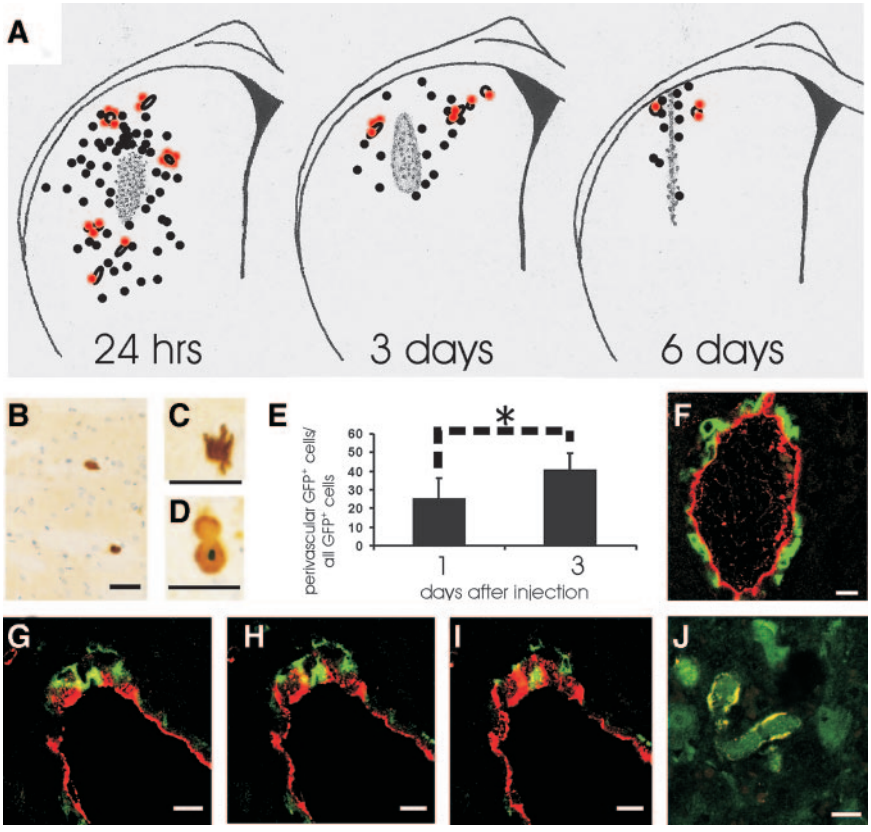

Figure 4. MicDCs disperse from the injection site into the parenchyma and to the perivascular space. GFP$^+$ micDCs were injected in a volume of 0.3 μl into the striatum of Lewis rats. Histological analyses were then made at different timepoints after the injection. **A:** Analysis of the location of GFP$^+$ micDCs at different time points after the injection into the striatum. Three-micron serial sections through the striatum of three individual animals were made 24 hours, 3 days, and 6 days after the injection. Every 10th section was stained with anti-GFP antibodies, and the location of each GFP$^+$ micDCs found within these sections was projected as a dot into the relevant scheme. Cells are found in the needle tract (small dots), in the parenchyma (black dots), and in the perivascular space (red dots). Please note that the injected cells disperse through the parenchyma (**B, C**), and that some of these cells undergo apoptosis (**D**). The parenchymal micDCs were often round (**B, D**), and had occasionally small processes (**C**). **E:** The ratio of the perivascular GFP$^+$ cells/all GFP$^+$ cells in the tissue increases over time. Shown here are the mean ratios ± SD after 1 and 3 days (10 animals per time point, pooled from three independently performed experiments). The difference between both groups is statistically significant at the 95% confidence interval (Mann Whitney W test, $^*P = 0.0058$). **F:** Confocal microscopy reveals many MHC class II$^+$ micDCs (OX-6 staining, green) in close vicinity to blood vessels (vWF staining, red). **G–I:** Stack of three confocal microscopy pictures, spaced 1 μm apart. This series of pictures shows the same MHC class II$^+$ micDCs (OX-6, green), which directly contacts the lumen of a blood vessel (vWF, red) and which is integrated within the blood vessel endothelium. **J:** MicDCs (GFP, green) in the lumen of blood vessels (vWF, yellow). Scale bars = 50 μm (**B**), 25 μm (**C, D**) and 10 μm (**F–J**).

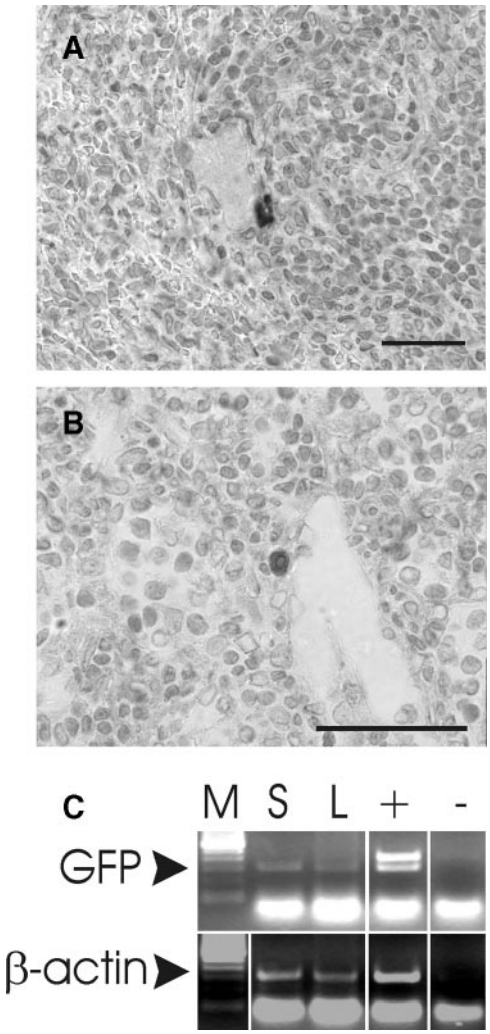

Figure 5. MicDCs in lymphoid organs. Three-micron thick serial sections of spleens (**A**) and mesenteric lymph nodes (**B**) isolated 3 days after the injection of micDCs into the striatum. The sections were stained with an anti-GFP antibody and searched for the presence of GFP^+ micDCs. GFP^+ micDCs appear brown. GFP^+ micDCs were found in the spleen, at the border between white and red pulp (**A**), and in the medulla of mesenteric lymph nodes (**B**). To further substantiate these findings, we performed PCR analysis of spleens (S, pooled from four animals) and lymph nodes (L, pooled from four animals) together with ear-derived cDNA from a GFP^+ Lewis rat as positive control (+) and omission of cDNA from the PCR reaction as negative control (−). The signal of the GFP products was very weak. We therefore made non-linear adjustments to make the PCR product visible on the picture, and to show that the GFP message was clearly detectable in spleens and lymph nodes (**C**). Scale bars = 100 μm.

lated GFP^+ microglial cells (Figure 6 hours), and injected them into the striatum of wild-type Lewis rats. Also in these cases, the injected cells were found in the parenchyma (Figure 6I). The injected cells were fully functional, as evidenced by the engulfment of erythrocytes near the needle tract (Figure 6J). Some of the cells were apoptotic (3 days after the injection, 14.3% of all GFP^+ microglial cells had condensed or fragmented nuclei as seen in Figure 6K). Again, we found evidence for perivascularly located GFP^+ cells. However, the numbers of these GFP^+ microglial cells was much lower than the number observed after injection of micDCs (Figure 6M) or bmDCs, and it remained constant over time (Figure 6L). We did not observe any GFP^+ microglial cells within the endothelium or the blood vessel lumen, and we were also unable to detect GFP^+ microglial cells in lymph nodes and spleens of the injected animals by PCR reactions (data not shown).

T Cell Infiltration as a Possible Trigger for MicDCs and BmDCs Emigration?

An emigration of myeloid cells from the *intact* CNS has not yet been described, which could indicate that this process might be initiated by a pathological trigger, eg, CNS inflammation. Is there evidence for T cell infiltration after the microinjection of cells into the striatum? To address this question, we stained the brain sections with W3/13 to search for CNS infiltrating T cells. We detected these cells in the perivascular space and in the parenchyma of the injected part of the striatum, but not in the contralateral, non-manipulated area of the striatum (Figure 7).

CNS-Emigrant DCs—Antigen Presenters in Vivo?

In further experiments, we searched for evidence of whether CNS emigrant micDCs were able to provoke antigen-specific immune reactions in the peripheral immune system. Since there are no transgenic rats available that carry large numbers of naive, CNS-antigen specific T cells in their immune repertoire (as would be the case, eg, for MBP-reactive T cell receptor transgenic mice[37]), we decided to search for reactivation of MBP-specific memory T cells that had been introduced into the peripheral immune system of the animals at the time of the intrastriatal injection of the micDCs. Although we tried several different experimental setups (ie, search for proliferation of CFSE-labeled MBP-specific T cells by FACS; search for the expansion of MBP-specific T cells by ELISPOT and T cell proliferation assays; and search for direct physical interaction between Cell tracker orange labeled MBP-specific T cells and GFP^+ emigrated micDCs in the spleen), we were unable to demonstrate any interactions between these different types of cells, probably due to the extremely low numbers of emigrated micDCs. Hence, with the animal model used, it remains open as to whether CNS emigrant DCs are antigen presenters *in vivo*. Is there any evidence that the injected DCs do interact *in vivo* at all with T cells? To answer this question, we searched for evidence of physical contact between GFP^+ DCs and T cells at the injection site. We found close contact between T cells and micDCs as well as bmDCs, both in the striatal parenchyma and in the perivascular space (Figure 8).

Discussion

For a long time, drainage of tissue-resident DCs by lymphatic vessels was considered to be the prototypic migratory pathway of these cells. The brain lacks such a classical lymphatic drainage.[10] Moreover, it has been

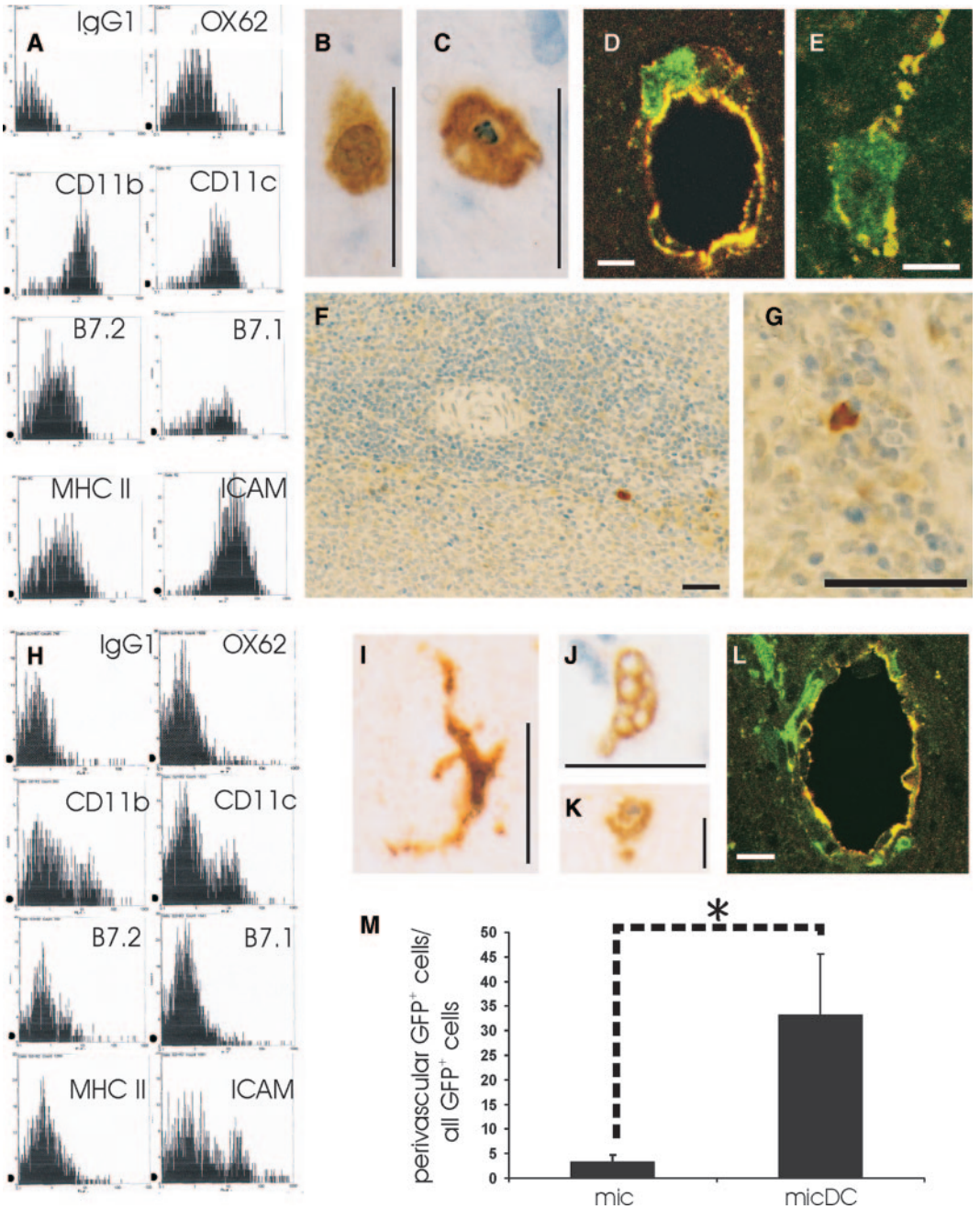

Figure 6. The migratory behavior of bmDCs and microglia. Flow cytometric analysis of surface marker expression (**A**) of GFP$^+$ bmDCs. The cells are characterized by a strong surface expression of MHC class II products and ICAM-1. GFP$^+$ bmDCs were injected in a volume of 0.3 μl into the striatum of Lewis rats. Histological analyses were then made at different time points after the injection. The injected cells disperse through the parenchyma (**B**). Some of these cells undergo apoptosis (**C**). Confocal microscopy reveals GFP$^+$ micDCs (green) in close vicinity to blood vessels (vWF staining, yellow; **D**) and also in the blood vessel lumen (**E**). We also found GFP$^+$ bmDCs in the spleen, again at the border of the red/white pulp (**F, G**). Flow cytometric analysis of surface marker expression (**H**) of GFP$^+$ microglial cells. The cells are characterized by an almost complete absence of surface MHC class II products and costimulatory molecules. GFP$^+$ microglial cells were injected in a volume of 0.3 μl into the striatum of Lewis rats. Histological analyses were then made at different timepoints after the injection. The injected cells are able to acquire the typical ramified microglial morphology and are also seen in the parenchyma (**I**). Some of them engulf erythrocytes at the injection site (**J**). Also apoptotic GFP$^+$ microglial cells can be found (**K**). Confocal microscopy revealed GFP$^+$ micDCs (green) in close vicinity to blood vessels (vWF staining, yellow). An example of such a blood vessel is shown in (**L**). The ratio of perivascular GFP$^+$ cells/all GFP$^+$ cells in the tissue is lower in the group of injected microglial cells than in the case of the injected micDCs. Shown here are the mean ratios ± SD. **M:** For each group, data were pooled from days 1 and 3. Group sizes were $n = 5$ (mic) and $n = 20$ (mic DC). The difference between both groups is statistically significant at the 95% confidence interval (Mann Whitney W test, $^*P = 0.00077$). Scale bars = 10 μm (**D, E, L**), 25 μm (**B, C, I, J, K**), and 50 μm (**F, G**).

described that antigens injected into the brain drain to the B cell zones of deep cervical lymph nodes,[11] that bone marrow-derived DCs injected into the corpus callosum remain mostly confined around the injection site or migrate only a short distance along the adjacent white matter tracts,[12] and that bone marrow-derived DCs injected into the cerebrospinal fluid contained within the lateral ventricle reach only the B cell follicles of cervical

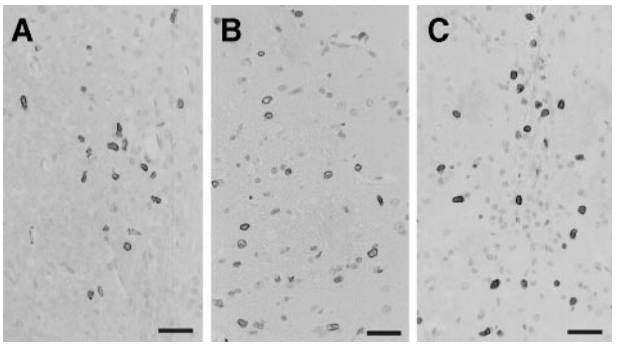

Figure 7. T cell infiltration at the injection site. Histological staining using the W3/13 antibody to reveal T cells in the striatum, 1 (**B, C**) or 3 (**A**) days after the injection of micDCs (**A**), bmDCs (**B**), and microglial cells (**C**). T cells ($W3/13^+$, dark) were seen at the injected site, close to the needle tract and within the parenchyma, but were absent from the contralateral unmanipulated site. Scale bars = 50 μm.

lymph nodes.[12] Therefore, it was concluded that DCs from the brain show a peculiar migratory behavior and are unable to enter other lymphatic organs.[12] We show here that micDCs and bmDCs, but not microglial cells, that have been injected into the striatum can leave the CNS via the blood stream and can enter mesenteric lymph nodes and spleen.

In terms of their route of exit from the CNS, and in terms of their function as antigen presenting cells, micDCs and bmDCs are remarkably similar. These cells differ, however, in their location during maturation: Microglia-derived dendritic cells differentiate within the CNS parenchyma,[5,6] while bone marrow-derived dendritic cells mostly mature within the perivascular space.[7,8] Although not formally shown in our study, these two compartments could differ from each other in the availability of antigenic peptides and could yield to dendritic cells that might activate T cells with different CNS antigen specificities following their (re-)entry into the peripheral immune system.

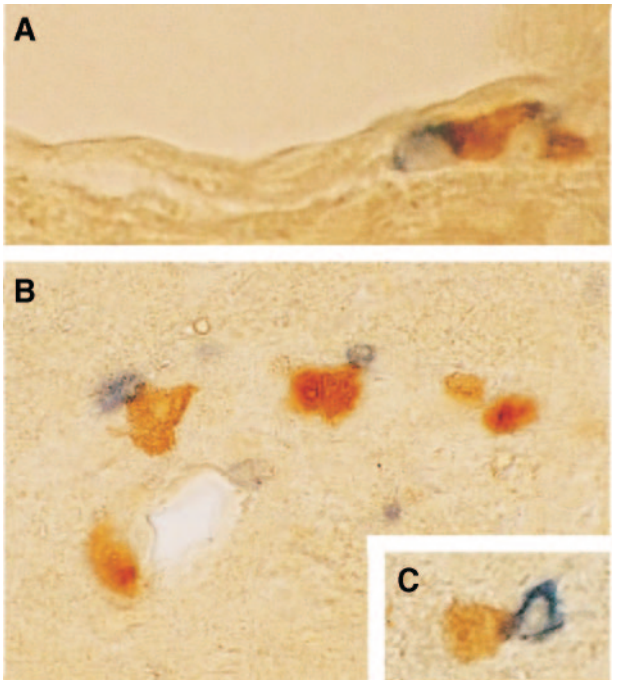

Figure 8. Interactions between dendritic cells and T cells at the injection site. Histological staining using the W3/13 antibody to reveal T cells (blue) in the striatum and the anti-GFP antibody to detect injected micDCs and bmDCs (brown). Shown here are intercellular contacts between micDCs and T cells (**A**, perivascular space, 3 days after the injection; **C**, parenchyma, 24 hours after the injection), and between bmDCs and T cells (**B**, parenchyma, 3 days after the injection).

Our findings that dendritic cells can leave the CNS via the blood stream raise two specific questions:

(1) why was this migratory pattern not observed earlier, by other studies? and

(2) what is the significance of our findings for the understanding of the onset and/or progression of autoimmune CNS diseases like multiple sclerosis or experimental autoimmune encephalomyelitis?

In an attempt to address the first question, we carefully analyzed the injection procedures applied by the different studies. We found that the other studies on antigen and cellular drainage from the CNS were performed using rather large volumes of material deposited at the injection sites, ranging from 2 × 20 μl injected into the frontal lobe,[38] 10 μl injected into the corpus callosum or the lateral ventricle,[12] down to 2 × 0.75 μl injected into the caudate nuclei.[39] Since the reported interstitial fluid bulk flow rate in the rat brain is in the range of 0.1 to 0.3 μl/min/g,[40] these deposits might represent supraphysiological amounts of fluid containing antigens or cells that could have saturated the available space at the injection site, resulting in a robust spillover into interstitial fluid/cerebrospinal fluid drainage pathways. In marked contrast, our inoculum had a total volume of 1 × 0.3 μl, and was hence much more within the range of the physiological interstitial flow rate. Thus, we minimized both the spill-over to the CSF compartment and the tissue damage at the injected site. Although we cannot formally exclude that some of the injected DCs found in the spleens or mesenteric lymph nodes had entered the blood stream as a result of the injection trauma, several lines of evidence strongly suggest that brain-derived DCs can indeed actively leave the CNS via the blood stream: First, we observed a migration of the injected DCs from the CNS parenchyma to the perivascular space, an integration of the migrated cells into the endothelium lining of the CNS vasculature, and the presence of these cells in the lumen of blood vessels days after the injection into the striatum. Secondly, i.v. injection of *ex vivo* expanded bone marrow-derived DCs also resulted in the accumulation of DCs in the lung and the T cell zones of mesenteric lymph nodes, Peyer's patches, spleen and thymus in one study,[13] and in the lung, liver, spleen and bone marrow in a second study.[14] The latter study also established that immature DCs deposited in the footpads of mice could be recovered from the blood and the draining lymph nodes following the induction of maturation by LPS stimulation.[14] And last, it has been repeatedly described that tissue-resident DCs are able to reach the spleen[15–18] (and the only way to do so is by re-entering the circulation[14]), that transplanted graft-derived DCs rapidly ap-

pear in the recipient's blood and spleen,[19,20] and that gut derived DCs appear in the blood after intragastric infections.[21] Based on these observations we conclude that brain-derived DCs behave essentially like any other tissue-derived DCs. The most important factors triggering maturation and exit of tissue-resident DCs are infection and inflammation.[21,41] Interestingly, in our experimental animals, the presence of $CD3^+$ T cells at the striatal injection site strongly suggests enhanced T cell influx/low grade inflammation at this site, which could provoke the formation of a migration-permissive microenvironment. A similarly migration-permissive environment is probably also created in the context of large scale CNS inflammation in human patients with multiple sclerosis[8,19] and in animals with experimental autoimmune encephalomyelitis[9] where inflammation is typically associated with an accumulation of DCs in the meninges or in the perivascular cuffs centering demyelinating lesions. In SJL mice with EAE, the encounter of DCs with blood-derived naive T cells in perivascular cuffs is the dominant, and perhaps even the only, possibility to activate a pathogenic T cell population that drives epitope spreading and clinical relapses.[9,42] It remains open whether this is the only mechanism triggering relapses and epitope spreading cascades observed in multiple sclerosis patients,[8,43] since the homing of brain-derived DCs to lymphatic organs could provide a further element of risk leading to the *de novo* induction of CNS antigen-specific T cell responses, and to the reactivation of CNS antigen-specific memory T cell responses. Both naive and memory T cells are found in lymph nodes and spleens,[44–46] and might even significantly differ from each other in their requirements for activation by DCs.[45,47,48,14] It also remains unresolved whether the homing of brain-derived DCs to lymphatic organs triggers CNS immunity at all. Alternatively, it could provide a mechanism for the effective down-regulation of tissue specific autoimmune responses, since both semimature and mature DCs are migratory but differ in their T cell activation patterns: Semimature DCs are actively tolerogenic and induce antigen-specific IL-10–producing $CD4^+$ regulatory T cells, while mature DCs are unable to mediate tolerance and induce T cell immunity instead.[34]

Tissue-resident DCs were repeatedly shown to carry fluorescent beads, dyes, or antigens to the spleen,[15–18] and the DCs derived from our cultures readily take up antigens like FITC-dextran and FITC-BSA. Unfortunately, in the present study, we were unable to clarify whether and to which extent CNS-derived DCs contribute to the onset or progression of autoimmune CNS disease: Since the number of brain-derived DCs found in the spleens and lymph nodes after intrastriatal injections of micDCs and bmDCs is extremely low, we would need a suitable transgenic rat model harboring sufficiently large numbers of CNS antigen-specific naive T cells in the body to show whether or not these DsC are able to activate CNS antigen-specific memory T cells outside the CNS. Further studies are needed to specifically address these issues.

Acknowledgments

We thank Marianne Leisser, Ulli Köck and Angela Kury for technical assistance, Dr. Johannes Stöckl (Institute for Immunology, Medical University Vienna) for use of the β-counter, Dr. Roland Grundtner for being our "blinded observer," and Drs Carlos Lois and David Baltimore (California Institute of Technology, Pasadena, California) for initial breeders of GFP transgenic rats.[49]

References

1. McMenamin PG: Distribution and phenotype of dendritic cells and resident tissue macrophages in the dura mater, leptomeninges, and choroid plexus of the rat brain as demonstrated in wholemount preparations. J Comp Neurol 1999, 405:553–562
2. McMenamin PG, Wealthall RJ, Deverall M, Cooper SJ, Griffin B: Macrophages and dendritic cells in the rat meninges and choroid plexus: three-dimensional localization by environmental scanning electron microscopy and confocal microscopy. Cell Tissue Res 2003, 313:259–269
3. Kivisäkk P, Mahad DJ, Callahan MK, Sikora K, Trebst C, Tucky B, Wujek J, Ravid R, Staugaitis SM, Lassmann H, Ransohoff RM: Expression of CCR7 in multiple sclerosis: implications for CNS immunity. Ann Neurol 2004, 55:627–638
4. Henkel JS, Engelhardt JI, Siklos L, Simpson EP, Kim SH, Pan T, Goodman JC, Siddique T, Beers DR, Appel SH: Presence of dendritic cells. MCP-1, and activated microglia/macrohages in amyotrophic lateral sclerosis spinal cord tissue Ann Neurol 2003, 55:221–235
5. Fischer HG, Bonifas U, Reichmann G: Phenotype and functions of brain dendritic cells emerging during chronic infection of mice with Toxoplasma gondii. J Immunol 2000, 164:4826–4834
6. Reichmann G, Schroeter M, Jander S, Fischer HG: Dendritic cells and dendritic-like microglia in focal cortical ischemia of the mouse brain. J Neuroimmunol 2002, 129:125–132
7. Serafini B, Columba-Cabezas S, Di Rosa F, Aloisi F: Intracerebral recruitment and maturation of dendritic cells in the onset and progression of experimental autoimmune encephalomyelitis. Am J Pathol 2000, 157:1991–2002
8. Serafini B, Rosicarelli B, Magliozzi R, Stigliano E, Capello E, Mancardi GL, Aloisi F: Dendritic cells in multiple sclerosis lesions: maturation stage, myelin uptake, and interaction with proliferating T cells. J Neuropathol Exp Neurol 2006, 65:124–141
9. Bailey SL, Schreiner B, McMahon E, Miller SD: CNS myeloid DCs presenting endogenous myelin peptides "preferentially" polarize CD4+ TH-17 cells in relapsing EAE. Nat Immunol 2007, 8:172–180
10. Bradl M, Flugel A: The role of T cells in brain pathology. Curr Top Microbiol Immunol 2002, 265:141–162
11. Cserr HF, Harling-Berg CJ, Knopf PM: Drainage of brain extracellular fluid into blood and deep cervical lymph and its immunological significance. Brain Pathol 1992, 2:269–276
12. Hatterer E, Davoust N, Didier-Bazes M, Vuaillat C, Malcus C, Belin M-F, Nataf S: How to drain without lymphatics? Dendritic cells migrate from the cerebrospinal fluid to the B-cell follicles of cervical lymph nodes. Blood 2006, 107:806–812
13. Schimmelpfennig CH, Schulz S, Arber C, Baker J, Tarner I, McBride J, Contag CH, Negrin RS: Ex vivo expanded dendritic cells home to T-cell zones of lymphoid organs and survive in vivo after allogeneic bone marrow transplantation. Am J Pathol 2005, 167:1321–1331
14. Cavanagh LL, Bonasio R, Mazo IB, Halin C, Cheng G, van der Velden AWM, Cariappa A, Chase C, Russell P, Starnbach MN, Koni PA, Pillai S, Weninger W, von Adrian UH: Activation of bone marrow-resident memory T cells by circulating, antigen-bearing dendritic cells. Nat Immunol 2005, 6:1029–1037
15. Randolph GJ, Inaba K, Robbiani DF, Steinman RM, Muller WA: Differentiation of phagocytic monocytes into lymph node dendritic cells in vivo. Immunity 1999, 11:753–761
16. Mullins DW, Sheasley SL, Ream RM, Bullock TN, Fu YX, Engelhard VH: Route of immunization with peptide-pulsed dendritic cells controls the distribution of memory and effector T cells in lymphoid

tissues and determines the pattern of regional tumor control. J Exp Med 2003, 198:1023–1034
17. Enioutina EY, Visic D, Daynes RA: The induction of systemic and mucosal immune responses to antigen-adjuvant compositions administered into the skin: alterations in the migratory properties of dendritic cells appears to be important for stimulating mucosal immunity. Vaccine 2000, 18:2753–2767
18. Racanelli V, Behrens SE, Aliberti J, Rehermann B: Dendritic cells transfected with cytopathic self-replicating RNA induce crosspriming of CD8+ T cells and antiviral immunity. Immunity 2004, 20:47–58
19. Ambrosini E, Remoli ME, Giacomini E, Rosicarelli B, Serafini B, Lande R, Aloisi F, Coccia EM: Astrocytes produce dendritic cell-attracting chemokines in vitro and in multiple sclerosis lesions. J Neuropathol Exp Neurol 2005, 64:706–715
20. Saiki T, Ezaki T, Ogawa M, Matsuno K: Trafficking of host- and donor-derived dendritic cells in rat cardiac transplantation: allosensitization in the spleen and hepatic nodes. Transplantation 2001, 71:1806–1815
21. Vazquez-Torres A, Jones-Carson J, Bäumler AJ, Falkow S, Valdivia R, Brown W, Le M, Berggren R, Parks WT, Fang FC: Extraintestinal dissemination of Salmonella by CD18-expressing phagocytes. Nature 1999, 401:804–808
22. Giulian D, Baker TJ: Characterization of ameboid microglia isolated from developing mammalian brain. J Neurosci 1986, 6:2163–2178
23. Grauer O, Wohlleben G, Seubert S, Weishaupt A, Kämpgen E, Gold R: Analysis of maturation states of rat bone marrow-derived dendritic cells using an improved culture technique. Histochem Cell Biol 2002, 117:351–362
24. Aboul-Enein F, Bauer J, Klein M, Schubart A, Flugel A, Ritter T, Kawakami N, Siedler F, Linington C, Wekerle H, Lassmann H, Bradl M: Selective and antigen-dependent effects of myelin degeneration on central nervous system inflammation. J Neuropathol Exp Neurol 2004, 63:1284–1296
25. Talmor M, Mirza A, Turley S, Mellmann I, Hoffman LA, Steinman RM: Generation or large numbers of immature and mature dendritic cells from rat bone marrow cultures. Eur J Immunol 1998, 28:811–817
26. Shortman K, Liu Y-J: Mouse and human dendritic cell subsets. Nat Rev Immunol 2002, 2:151–161
27. de la Mata M, Riera CM, Iribarren P: Identification of a CD8a+ dendritic cell subpopulation in rat spleen and evaluation of its OX-62 expression. Clin Immunol 2001, 101:371–378
28. León B, Martinez del Hoyo G, Parrillas V, Vargas HH, Sánchez-Mateos P, Longo N, López-Bravo M, Ardavin C: Dendritic cell differentiation potential of mouse monocytes: monocytes represent immediate precursors of CD8- and CD8+ splenic dendritic cells. Blood 2004, 103:2668–2676
29. Vremec D, Shortman K: Dendritic cell subtypes in mouse lymphoid organs. Cross-correlation of surface markers, changes with incubation and differences among thymus, spleen and lymph nodes. J Immunol 1997, 159:565–573
30. Anderson KL, Perkin H, Surh CD, Venturini S, Maki RA, Torbett BE: Transcription factor PU. 1 is necessary for development of thymic and myeloid progenitor-derived dendritic cells. J Immunol 2000, 164:1855–1861
31. Guerriero A, Langmuir PB, Spain LM, Scott EW: PU. 1 is required for myeloid-derived but not lymphoid-derived dendritic cells. Blood 2000, 95:879–885
32. Schotte R, Nagasawa M, Weijer K, Spits H, Blom B: The ETS transcription factor Spi-B is required for human plasmacytoid dendritic cell development. J Exp Med 2004, 200:1503–1509
33. Schotte R, Rissoan MC, Bendriss-Vermare N, Bridon JM, Duhen T, Weijer K, Brière F, Spits H: The transcription factor Spi-B is expressed in plasmacytoid DC precursors and inhibits T, B, and NK-cell development. Blood 2003, 101:1015–1023
34. Lutz MB, Schuler G: Immature, semi-mature and fully mature dendritic cells: which signals induce tolerance or immunity? Trends Immunol 2002, 23:445–449
35. Floden AM, Combs CK: Microglia repetitively isolated from in vitro mixed glial cultures retain their initial phenotype. J Neurosci Methods 2007, 164:218–224
36. Matyszak MK, Perry VH: The potential role of dendritic cells in immune-mediated inflammatory diseases in the central nervous system. Neuroscience 1996, 74:599–608
37. Lafaille J, Nagashima K, Katsuki M, Tonegawa S: High incidence of spontaneous autoimmune encephalomyelitis in immunodeficient anti-myelin basic protein T cell receptor mice. Cell 1994, 78:399–408
38. Ling C, Sandor M, Fabry Z: In situ processing and distribution of intracerebrally injected OCA in the CNS. J Neuroimmunol 2003, 141:90–98
39. Gordon LB, Knopf PM, Cserr HF: Ovalbumin is more immunogenic when introduced into brain or cerebrospinal fluid than into extracerebral sites. J Neuroimmunol 1992, 40:81–87
40. Abbott NJ: Evidence for bulk flow of brain interstitial fluid: significance for physiology and pathology. Neurochem Int 2004, 45:545–552
41. Léon B, López-Bravo M, Ardavin C: Monocyte-derived dendritic cells formed at the infection site control the induction of protective T helper 1 responses against Leishmania. Immunity 2007, 26:390–392
42. McMahon EJ, Bailey SL, Castenada CV, Waldner H, Miller SD: Epitope spreading initiates in the CNS in two mouse models of multiple sclerosis. Nat Med 2005, 11:335–339
43. Tuohy VK, Yu M, Yin L, Kawczak JA, Johnson JM, Mathisen PM, Weinstock-Guttman B, Kinkel RP: The epitope spreading cascade during progression of experimental autoimmune encephalomyelitis and multiple sclerosis. Immunol Rev 1998, 164:93–100
44. Villadangos JA, Heath WR: Life cycle, migration and antigen presenting functions of spleen and lymph node dendritic cells: limitaitons of the Langerhans cells paradigm. Seminars Immunol 2005, 17:262–272
45. Belz GT, Bedoui S, Kupresanin F, Carbone FR, Heath WR: Minimal activation of memory CD8+ T cell by tissue-derived dendritic cells favors the stimulation of naive CD8+ T cells. Nat Immunol 2007, 8:1060–1066
46. Flugel A, Berkowicz T, Ritter T, Labeur M, Jenne DE, Li Z, Ellwart JW, Willem M, Lassmann H, Wekerle H: Migratory activity and functional changes of green fluorescent effector cells before and during experimental autoimmune encephalomyelitis. Immunity 2001, 14:547–560
47. Croft M, Bradley LM, Swain SL: Naive versus memory CD4 T cell responses to antigen. Memory cells are less dependent on accessory cell costimulaiton and can respond to many antigen-presenting cell types including resting B cells. J Immunol 1994, 152:2675–2685
48. Byrne JA, Butler JL, Cooper MD: Differential activation requirements for virgin and memory T cells. J Immunol 1988, 141:3249–3257
49. Lois C, Hong EJ, Pease S, Brown EJ, Baltimore D: Germline transmission and tissue-specific expression of transgenes delivered by lentiviral vectors. Science 2002, 295:868–872